SEMARAK ILMU PUBLISHING

Advances in Fluid, Heat and Materials Engineering

Journal homepage:
https://semarakilmu.com.my/journals/index.php/afhme/index
ISSN: 3083-8134

CFD Analysis on Double Leaks of Subsea Pipeline Leakage

Asral[1], Ridwan Abdurrahman[1], Nurnabila Syuhada Azian[2], Ishkrizat Taib[2,*], Wu Shunfann[2], Yap Wee Hang[2], Yeap Swee Hong[2], Melchiades Joeffrey Jr[2], Feblil Huda[1], Awaludin Martin[1]

[1] Department of Mechanical Engineering, Universitas Riau, Pekanbaru 28293, Indonesia
[2] Faculty of Mechanical and Manufacturing Engineering, Universiti Tun Hussein Onn Malaysia, 86400 Parit Raja, Batu Pahat, Johor, Malaysia

ARTICLE INFO

Article history:
Received 7 March 2024
Received in revised form 27 April 2024
Accepted 23 May 2024
Available online 19 June 2024

Keywords:
Pipe leakage; computational fluid dynamic (CFD); velocity; leak detection; pressure; turbulence kinetic energy (TKE)

ABSTRACT

The transportation of materials through industrial pipelines is essential in many sectors. However, pipeline leakage is a common and potentially devastating issue, particularly in subsea environments. Although extensive research has been conducted on pipeline leak detection, the specific dynamics of double leaks in subsea pipelines under varying fluid velocities have not been thoroughly investigated. This study used numerical simulations with ANSYS FLUENT, based on the standard k–ε model under steady-state conditions, to examine the effects of fluid velocity on the leak flow rate, pressure distribution, and turbulence kinetic energy in double-leak subsea pipeline models. The results indicate that changes in pipeline fluid velocity have a minimal impact on the flow behaviour in the leak regions. Notably, the leak flow rate in the first leak consistently exceeded that in the second leak. The pressure around the leaks exhibits fluctuations owing to turbulence, which diminishes further from the leak points towards the pipe centreline. These findings suggest that leak detection systems should be positioned near the pipe surface to enhance the detection accuracy and effectiveness. This study provides valuable insights into the fluid dynamics of double leaks in subsea pipelines and contributes to improved leak management strategies.

1. Introduction

The use of industrial pipelines is becoming increasingly evident today because of the growing need to transport materials, often liquids, over long distances [1]. Pipelines are the primary means of collecting and transporting a wide range of commodities including oil, natural gas, chemicals, water, and sewage [2]. One of the main areas of research in duct engineering focuses on ensuring flow, particularly addressing fluid leakage, which is prone to occur because of corrosive environments to which ducts are often exposed. According to the Oxford Dictionary, leakage is defined as the accidental entry or escape of fluid through a hole or fissure in a pipe. Pipeline monitoring, control, operation, and maintenance are crucial activities that have evolved significantly. Fluid loss into the external environment can directly affect the velocity, pressure, and temperature fields of the pipeline and reduce the total volume delivered to the final destination [1].

* *Corresponding author.*
E-mail address: iszat@uthm.edu.my

https://doi.org/10.37934/afhme.1.1.1026

Pipeline leakage is a common phenomenon, often caused by third-party damage, geological hazards, accidents, human error during operation, poor workmanship, sudden changes in pressure, corrosive action, cracks, pipeline defects, joints in pipes or equipment, or lack of maintenance. The consequences of pipeline leakage can be enormous, if not addressed immediately and carefully. In addition to water pipelines, subsea pipelines are used to transport hydrocarbons and natural gas [3]. Failure of an oil transport pipeline due to a leak would result in an oil spill into the marine area, negatively impacting human health and marine life [4]. Regarding the pressure behaviour around the leak, a fully developed steady flow was driven by gravity or pressure forces in a constant-diameter pipe. Gravity does not significantly affect the horizontal pipe flow, except for the hydrostatic pressure variation across the pipe, which is usually insignificant. The pressure difference between the sections of the horizontal pipe forces fluid through the pipe [5].

For turbulence kinetic energy (TKE) behaviour around a leak, turbulence is an essential phenomenon that influences all atmospheric processes, particularly near the surface. Turbulence represents the irregularity or randomness of the flow. The existence of a spectral gap in the turbulence spectrum is important to separate the mean from the turbulent part of the flow. Turbulence influences the mean (nonturbulent) part of the flow through a specific mechanism called eddy flux [6]. The most important factors are buoyant production or consumption and shear production of the TKE, which vary significantly in time and space (especially in height). Additionally, dissipation is a crucial term because it reduces turbulence over time by dissipating energy from large to smaller vortices. In meteorology, the TKE is useful for parameterising sub-grid processes. Smaller-scale motions, namely turbulence, are not directly modelled. Instead, the effects of these sub-grid scales on the larger scales were approximated. These smaller-scale motions are parameterised using sub-grid-scale stochastic approximation or models. A low TKE value indicates better aerodynamic properties [7].

Timely leak detection and location identification are essential because the economic impact of a hydrocarbon leak on stakeholders can be significant. Pipeline leaks can negatively affect life, the environment, the economy, and corporate reputations. When operating in subsea areas, additional precautions must be taken, making rapid leak detection and location identification crucial. Conducting small-scale leakage experiments on subsea pipelines is difficult, mainly because the pipelines may need to release hydrocarbons into the environment [8-10].

Pipeline leak detection technologies play a key role in ensuring pipeline transport safety. It is important to detect and locate pipeline leaks promptly to reduce or minimise fluid losses in the pipeline [11]. There are four main categories of causes for pipeline leaks: operational, structural, unintentional, and intentional. The operational category includes leaks due to oil/gas pipeline operations such as human error and equipment failure. The structural problem category includes failures in pipelines, such as explosions, collapses, fatigue, fractures, buckling, corrosion, and ruptures. Unintentional damage is often caused by construction workers near the pipelines. In addition, intentional damage can result from terrorist attacks and vandalism/theft [12].

Currently, the industry primarily uses two categories of detection methods, static and dynamic. Sandberg *et al.,* [13] state that dynamic detection systems are more preferable because they can be applied to working pipelines, whereas static leak detection methods are only useful after the leakage has been detected. According to Adegboye *et al.,* [14] leak detection methods can be divided into three categories: hardware, software, and biological approaches.

Fluid thermodynamics cannot be accurately captured in a small-scale laboratory setting because of the large diameters of the industrial full-scale pipelines. Therefore, numerical simulations can provide a better understanding of the internal pipeline flow and the consequences of pipeline leakage at different scales, reducing the cost and number of experiments [15-17]. Commercially

available ANSYS FLUENT computational fluid dynamics software was used for this purpose. The ANSYS workbench provides an integrated design, meshing techniques, and large degrees of freedom for pre- and post-processing in the simulation of fluid flow in pipelines [18]. Its parallel processing capabilities also enable the computation of large, detailed meshes required to capture the intricate flow dynamics near the leaks.

This study investigated and analysed the effect of changes in fluid velocity on the leak flow rate, pressure distribution, and turbulence kinetic energy around the leakage points. A pipeline transportation failure due to a leak could result in the spill of harmful chemicals into the marine area, negatively impacting human health and marine life. It is of practical importance to promptly detect and locate pipeline leaks to reduce or minimise fluid losses. Therefore, simulations were conducted to investigate the effect of fluid velocity on the leak flow rate, pressure distribution, and turbulence kinetic energy in near-leak regions and to analyse these flow parameters in double-leak subsea pipeline models. The goal is to provide substantial and easily analysable feedback that can facilitate rapid leak detection, thereby minimising environmental damage and protecting marine ecosystems.

2. Methodology

2.1 Geometry Modelling

A pipe with a diameter of 0.322 m was modelled using SolidWorks software to represent the most commonly used pipe in oil and gas distribution networks. The pipe is 8m long, with two leaks located 4m and 6m from the inlet, as shown in Figures 1 and 2. Leaks were approximated as circular openings. These leaks are very small compared to real-life issues in oil and gas pipeline distribution networks, each having a diameter of 0.01m, as shown in Figure 3.

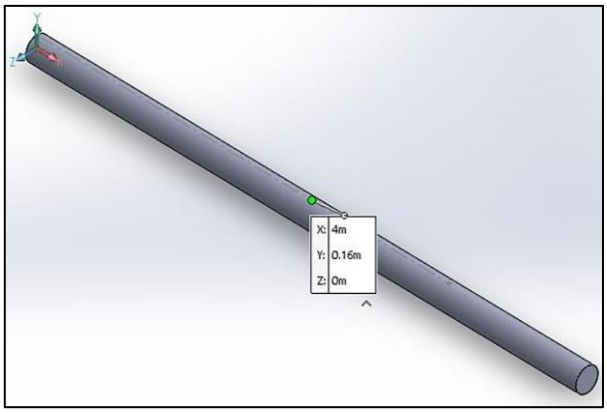

Fig. 1. Leak 1 location

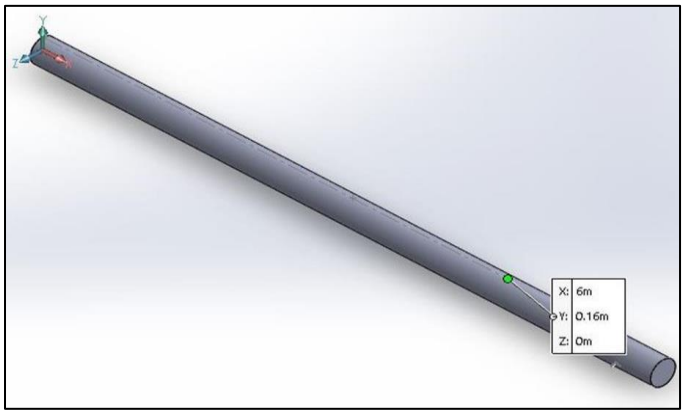

Fig. 2. Leak 2 location

Fig. 3. Circular leak diameter

2.2 Grid Independence Test

Meshing was performed, as illustrated in Figure 4. A grid independence test (GIT) was conducted to achieve precise and valid results in the CFD processor by minimising grid-induced truncation errors without compromising the results. This involved controlling the variation in element size and nodes [19, 20]. Table 1 lists the element size adjustments until the increment in the number of nodes becomes constant. The skewness and orthogonal values were within the acceptable range for a good mesh quality. The results were used to calculate the relative error using Eq. (1), and a velocity graph was plotted, as shown in Figure 5.

$$Relative\ error = \frac{Mesh_{n+1} - Mesh_n}{Mesh_n} X\ 100 \quad (1)$$

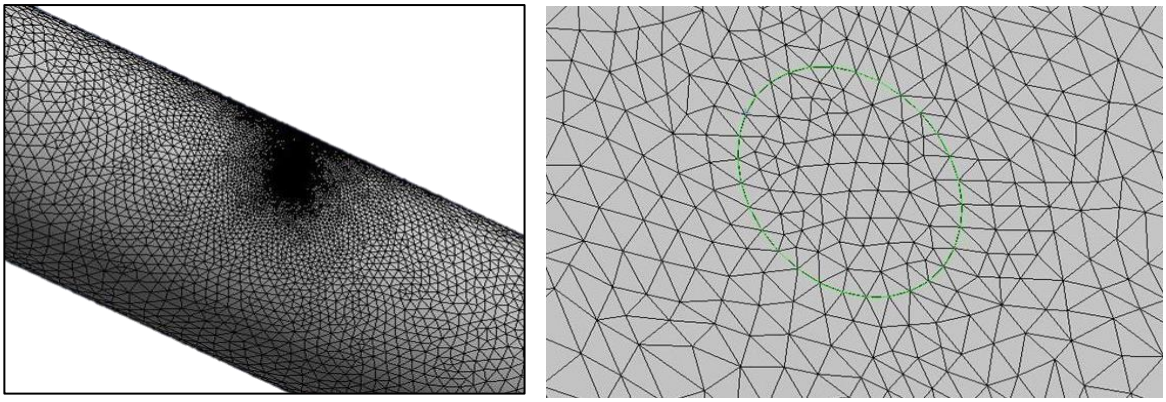

(a) (b)

Fig. 4. Meshing refinement of pipeline near the wall and leak (a) Normal view (b) Zoomed view

Table 1
Comparison of relative error

Division number(Pipe)	Division number (Leak)	Nodes number	Elements number	Max skewness	Min orthogonal	Velocity average	Relative error (%)
20	10	31014	171191	0.84203	0.15797	9.6109	-
40	20	80346	434711	0.79985	0.20015	9.5723	0.402
60	30	180276	979759	0.79902	0.20098	9.5607	0.121
80	40	338334	1849927	0.79875	0.20125	9.5672	0.068
100	50	549579	3018442	0.80420	0.19580	9.5607	0.068

There was a significant difference in the graph results between the 31,014-node mesh and other mesh node counts. The closest graphs were those for meshes with 180,276, 338,334, and 549,579 nodes. The chosen range of nodes used in this study was 180,276, which corresponds to an element count of 979,759.

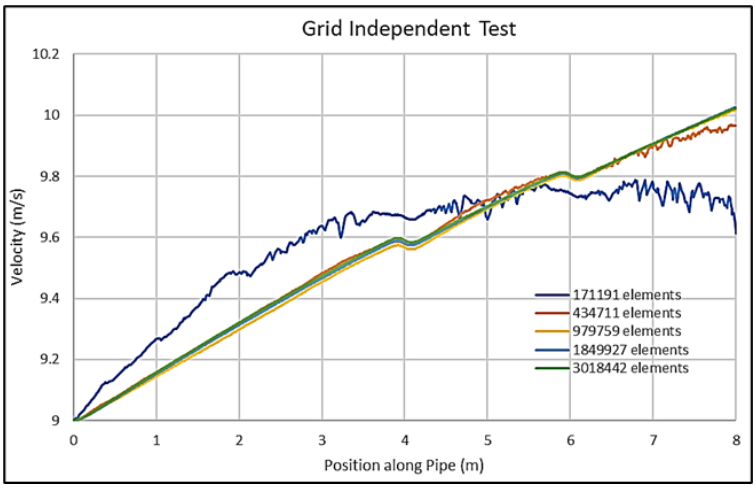

Fig. 5. Grid independent test

2.3 Governing Equations

The flow in the pipe exhibits general axial symmetry along the azimuthal direction, which can be described by a cylindrical coordinate system with all non-zero coordinates. As this is a turbulent study, Eqs. (2) and (3) are known as the Reynolds Averaged Navier-Stokes equations. The simulation was carried out at a constant density, assuming that water is an incompressible fluid flowing with a Mach number less than 0.3, and under steady-state conditions.

$$\frac{\partial u_j}{\partial x_j} = 0 \tag{2}$$

$$\frac{\partial(\rho u_i u_j)}{\partial x_j} = \frac{\partial p}{\partial x_i} + \frac{\partial}{\partial x_j}\left[\mu\left(\frac{\partial u_i}{\partial x_j} + \frac{\partial u_j}{\partial x_i}\right)\right] + \frac{\partial}{\partial x_j}\left(-\rho u'_i u'_j\right) \tag{3}$$

2.4 Boundary Conditions

Accurate modeling of real pipeline flow involves applying four key boundary conditions, as illustrated in Figure 6. At the inlet, a velocity condition was established based on typical Reynolds numbers for water, balancing flow requirements with the need to prevent pipe erosion. This ensures the model represents common water distribution systems accurately. For the main outlet, a pressure condition was used, creating a realistic pressure gradient along the pipe to mimic actual pipeline operations. Such realism is crucial for designing practical elements like pumps and valves.

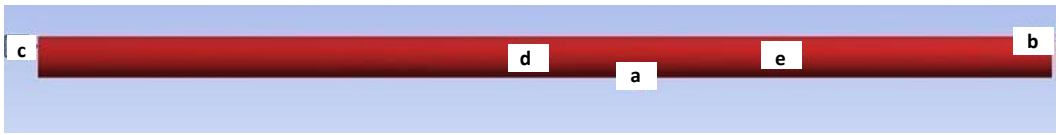

Fig. 6. Boundary condition in the model geometry (a) Pipe wall (b) Outlet (c) Inlet (d) Leak outlet 1 (e) Leak outlet 2

Leaks were modelled as pressure outlets at atmospheric pressure (zero gauge), simulating leaks in aboveground pipes or, in the subsea context, leaked into the ocean at a given depth. This condition is vital for understanding leak behaviour and its environmental impact. The boundary conditions for the flow model included a velocity inlet of 9 m/s, leak pressure outlets similar to the pressure 100 m

below sea level, which was 10.3421 bar (1034210 Pa), and a pressure outlet at the exit of the pipeline at 365.4221 bar (36542210 Pa).

The pipe walls were assigned a standard no-slip condition with predefined roughness to capture the effects of viscosity and wall friction. Additionally, the axial symmetry of the pipe flow was leveraged using cylindrical coordinates to simplify the model without losing accuracy in key areas, such as near leaks. These conditions create a model that accurately represents the physics of the leak pipeline. By realistically capturing inlet velocities, outlet pressures, leak conditions, and wall effects, the model provides a solid foundation for studying how leaks affect the pressure, velocity, and turbulence. Such insights are critical for developing leak detection algorithms and for assessing environmental risks, particularly in sensitive subsea environments.

2.5 Verification Data Process

The model geometry specifications were matched with those in a previous study by Wei and Masuri [4]. This allowed data verification between the current simulation and prior work. The verification ensures that the methodology is acceptable for different model geometries. As the error in the results was less than 5%, the desired geometry and properties were deemed acceptable. The errors were calculated using Eq. (4) and (5), respectively.

$$\text{Absolute error} = [\text{Journal similation-Verification simulation}] \tag{4}$$

$$\text{Relative error} = \frac{\text{Absolute error}}{\text{Journal simulation}} \times 100\% \tag{5}$$

3. Results

3.1 Data Verification

A comparison of the pressure along the pipe between the current simulation and a previous study by Wei and Masuri [4] is shown in Figure 7. The numerical data from the journal were digitised using a web application. For this simulation, a residual continuity value of 1×10^{-6} was set and the initialization involved 2000 iterations. Standard initialisation methods were used to initialise the flow field.

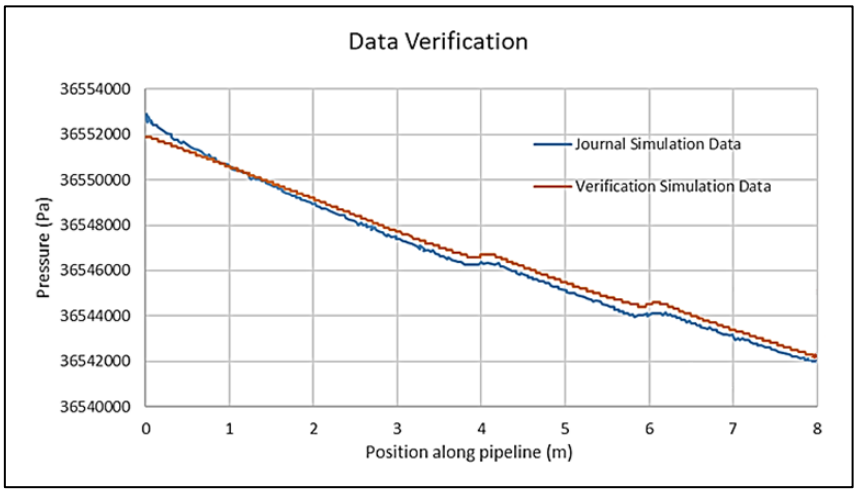

Fig. 7. CFD code verification with journal simulation

The average pressure for the verification simulation data is 36,546,680.43 Pa, whereas for the journal simulation data, it is 36,546,814.71 Pa. Calculating the relative error between these datasets using Eqs. (4) and (5) yields a relative error of 0.00037%. This indicates that the verification simulation data are valid because the relative error is below 5%.

3.2 Leak Flow Rate

The leak flow rate of the subsea pipeline model was identified and evaluated. Table 2 presents the leak flow rates at different fluid velocities. The leak flow rate increased as the fluid velocity increased for both leaks 1 and 2. However, the rate of increase in the leak flow rate at Leak 1 is slightly higher than at Leak 2, with an average increment of 4.16 X 10^{-4} L/s on Leak 1 and an average increment of 1.01 X 10^{-4} L/s of leak flow rate. Moreover, the leak flow rate in Leak 1 was always higher than that in Leak 2. Overall, changes in the fluid velocity at both Leaks 1 and 2 have only a small impact on the leak flow rate, as the difference is negligible.

Table 2
Leak flow rate for different fluid velocity at 3.6542 x 107 Pa

Velocity (m/s)	Leak flow rate (L/s)			
	Inlet	Outlet	Leak 1	Leak 2
6	486.82893	478.70191	4.0697605	4.0580829
7	567.96709	559.83877	4.0702382	4.0580706
8	649.10524	640.97631	4.0706578	4.0583115
9	730.2434	722.11401	4.0710069	4.0583853

3.3 Pressure Drops of Leaks at Different Fluid Velocities

The pressure drop at Leak 2 is much lower than that at Leak 1, as shown in Tables 3, 4, 5, and 6. According to the Bernoulli equation, the pressure is inversely proportional to velocity; when the velocity increases, the pressure decreases. Therefore, the pressure drop was much lower at Leak 2 than at Leak 1, as the velocity increased from the inlet to the end of the flow in the pipe. The pressure shifts are induced by the Bernoulli equation as the increase in velocity increases the flow rate toward the direction of the leaks. From the pattern of the value data, the consistency of the pressure drop in the area of leakage makes the pressure a reliable parameter for leak.

Table 3
Pressure drop value around leaks at v = 6m/s

Distance below leak (mm)	Pressure drop at Leak 1 (Pa)	Pressure drop at Leak 2 (Pa)
25	36543400.00	36542482.24
50	36544126.62	36543213.65
100	36544200.00	36543300.00
161 (centerline)	36544200.00	36543300.00

Table 4
Pressure drop value around leaks at v = 7m/s

Distance below leak (mm)	Pressure drop at Leak 1 (Pa)	Pressure drop at Leak 2 (Pa)
25	36544000.00	36542742.99
50	36544826.62	36543513.65
100	36544893.11	36543600.00
161 (centerline)	36544900.00	36543600.00

Table 5
Pressure drop value around leaks at v = 8m/s

Distance below leak (mm)	Pressure drop at Leak 1 (Pa)	Pressure drop at Leak 2 (Pa)
25	36544800.00	36543142.99
50	36545626.62	36543913.65
100	36545700.00	36544000.00
161 (centerline)	36545700.00	36544000.00

Table 6
Pressure drop value around leaks at v = 9m/s

Distance below leak (mm)	Pressure drop at Leak 1 (Pa)	Pressure drop at Leak 2 (Pa)
25	36545700.00	36543603.74
50	36546553.24	36544413.65
100	36544800.00	36543600.00
161 (centerline)	36544800.00	36544500.00

3.4 Study of Flow Behavior Around the Leaks
3.4.1 Flow behavior around the leaks at 6 m/s

The pressure distribution along the pipeline experiences a disturbance in the first and second leaks, as shown in Figure 8. The pressure change was almost similar for both leaks, with different pipeline pressures at the respective leaks. At 25 mm below the leak surface centreline, the pressure gradient signal was larger at the first leak than at the second leak. As the measurement moved away from the leak surface, the signal became negligible.

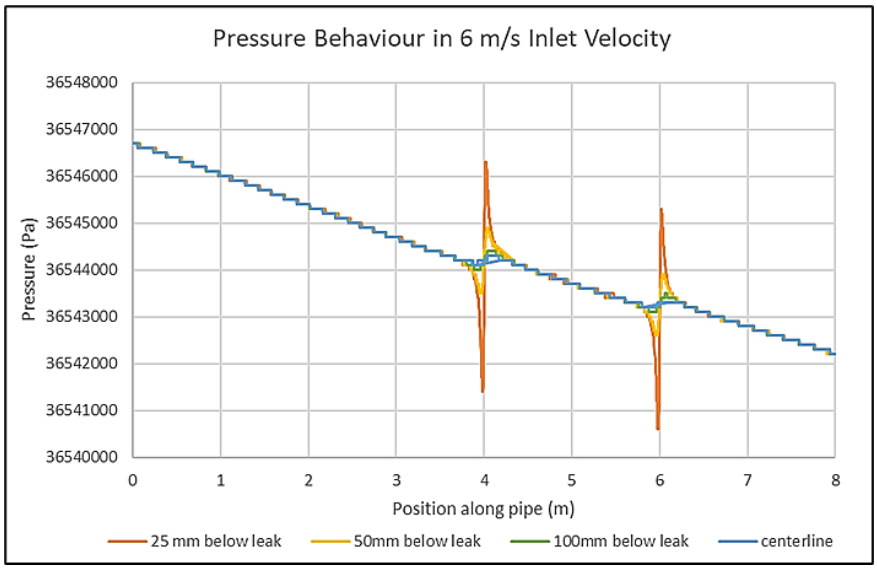

Fig. 8. Pressure distribution along pipeline for different positions at 6 m/s

The pressure gradient contour shows a sudden change in the pressure gradient in the leak regions, as illustrated in Figure 9. The extreme change in the pressure gradient ranges from 2.764 X 101 Pa/m at the entrance edge of the leak to 2.583 X 10^{10} Pa/m at the leak exit edge. The extreme value of the change in the pressure gradient signal can be used by leak detection systems to enhance the detection performance.

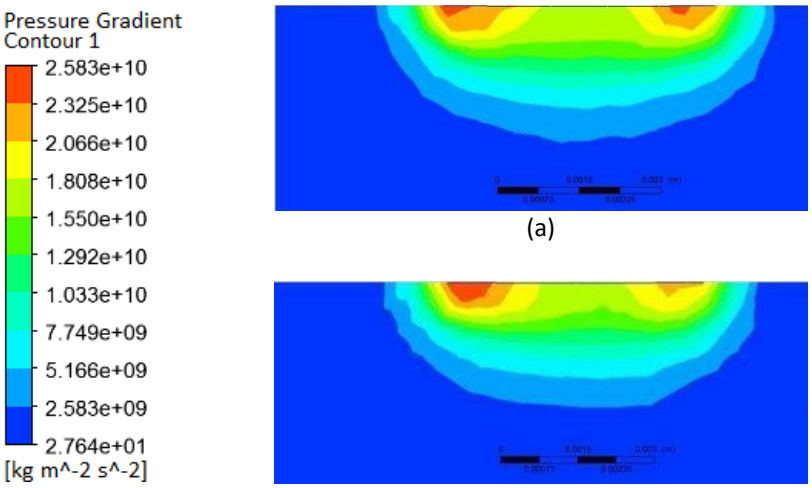

Fig. 9. Pressure gradient contour around leak region at 6 m/s (a) Leak 1 (b) Leak 2

Regarding the turbulence kinetic energy of the fluid flow in the leak region, the fluid experiences a sudden increase in the turbulence kinetic energy due to the leak. It increases from 2.644 x 10^{-4} J/kg, which is the turbulence kinetic energy of the pipeline flow, to 1.112 X 10^{4} J/kg near the leak and then decreases back to its initial value. Thus, turbulence kinetic energy can also serve as an assisting parameter in leak detection to avoid false-signal alarms (Figure 10).

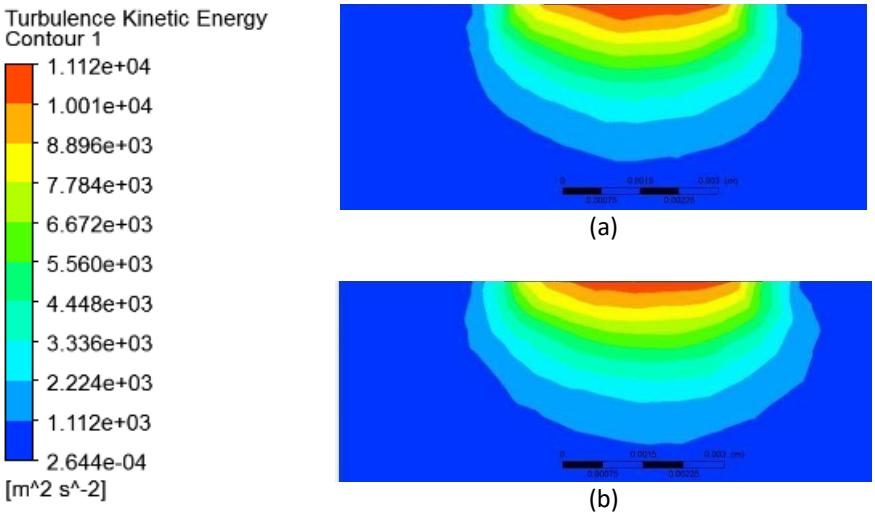

Fig. 10. Turbulence kinetic energy contour around leak region at 6 m/s (a) Leak 1 (b) Leak 2

3.4.2 Flow behavior around the leaks at 7 m/s

The pressure distribution along the pipeline experiences a disturbance in the first and second leaks, as shown in Figure 11. The pressure change is almost similar at both leaks, with different pipeline pressures at the respective leaks. At 25 mm below the leak surface centerline, the pressure gradient signal is larger at the first leak compared to the second leak. As the measurement moves away from the leak surface, the signal becomes hardly noticeable.

The pressure gradient contour shows a sudden change in the pressure gradient in the leak regions, as illustrated in Figure 12. The extreme change in the pressure gradient ranges from 1.582 X

10^1 Pa/m at the entrance edge of the leak to 2.574 X 10^{10} Pa/m at the exit edge of the leak. The extreme value of the change in the pressure gradient signal can be used by leak detection systems to enhance detection performance.

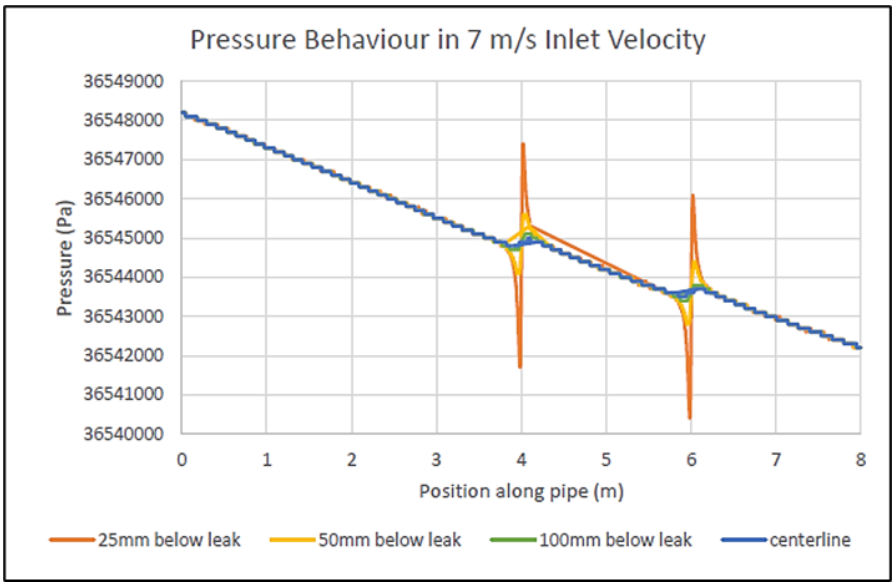

Fig. 11. Pressure distribution along pipeline for different positions at 7 m/s

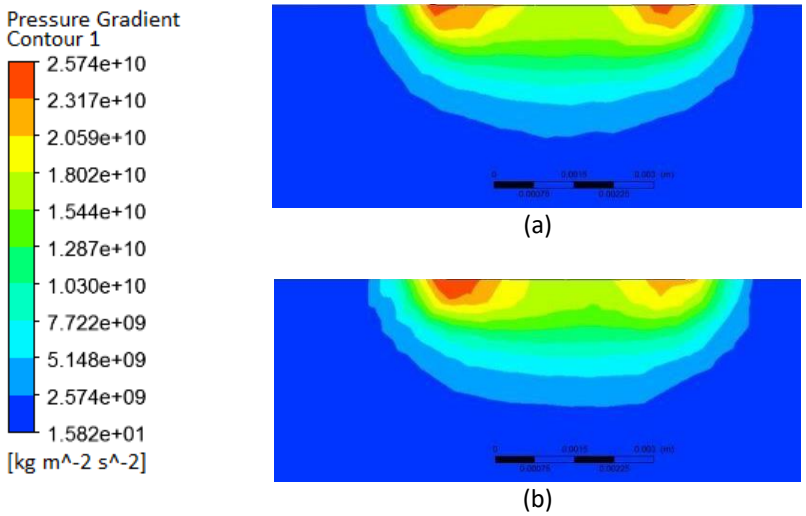

Fig. 12. Pressure gradient contour around leak region at 7 m/s (a) Leak 1 (b) Leak 2

Regarding the turbulence kinetic energy of fluid flow at the leak region, the fluid experiences a sudden increase in turbulence kinetic energy due to the leak. It increases from 3.106 x 10-4 J/kg, which is the turbulence kinetic energy of the pipeline flow to 1.109 x 104 J/kg near the leak and then decreases back to its initial value. Thus, turbulence kinetic energy can also serve as an assisting parameter in leak detection to avoid false-signal alarms (Figure 13).

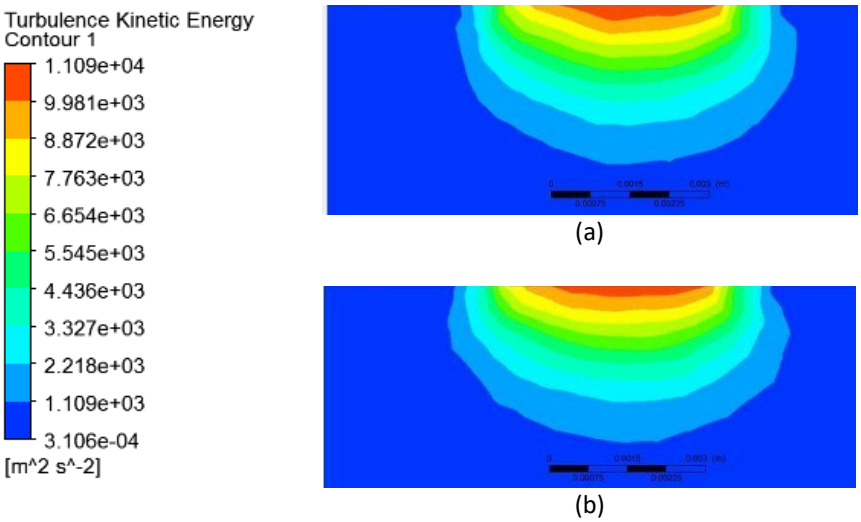

Fig. 13. Turbulence kinetic energy contour around leak region at 7 m/s (a) Leak 1 (b) Leak2

3.4.3 Flow behavior around the leaks at 8 m/s

First, the pressure distribution along the pipeline experienced disturbances at both Leaks 1 and 2, as shown in Figure 14. The distance between the two leaks is 2 m. However, the pattern of the pressure distribution was very similar for both the leaks.

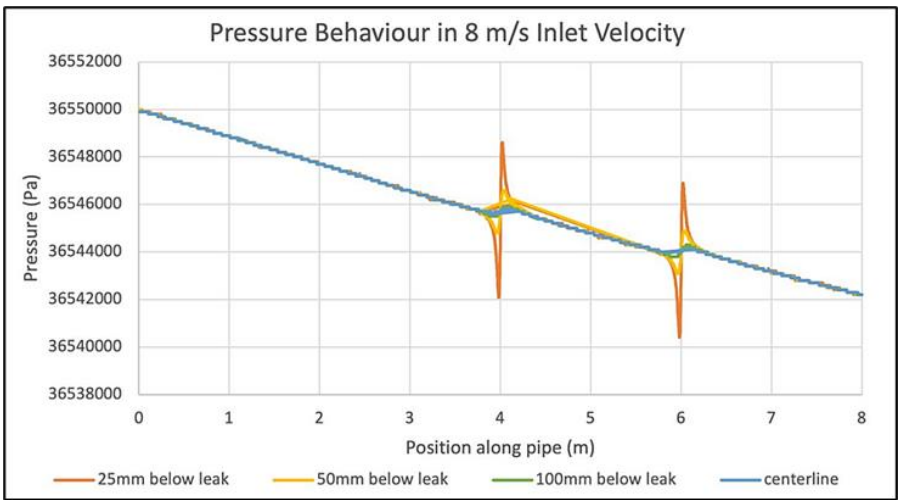

Fig. 14. Pressure distribution along pipeline for different positions at 8 m/s

From the above graph, the pressure behaviour 25 mm below the leak surface shows the largest change, resulting in the widest spike at both leaks. Conversely, the pressure behaviour at the centre of the pipeline (161 mm) had the smallest spike, indicating a slight pressure change around the leaks. This demonstrates that as the measurement moved away from the leak surface, the leakage signal became less noticeable.

From the pressure gradient contour in Figure 15, there is a sudden change of pressure around the leak region. The extreme change of pressure gradient has a range from 3.580 x 101 Pa/m to 2.573 x 1010 Pa/m at the entrance edge of leak and the exit edge of the leak, respectively. The pressure gradient can be used as the data for a leak detection system to enhance the performance of detection.

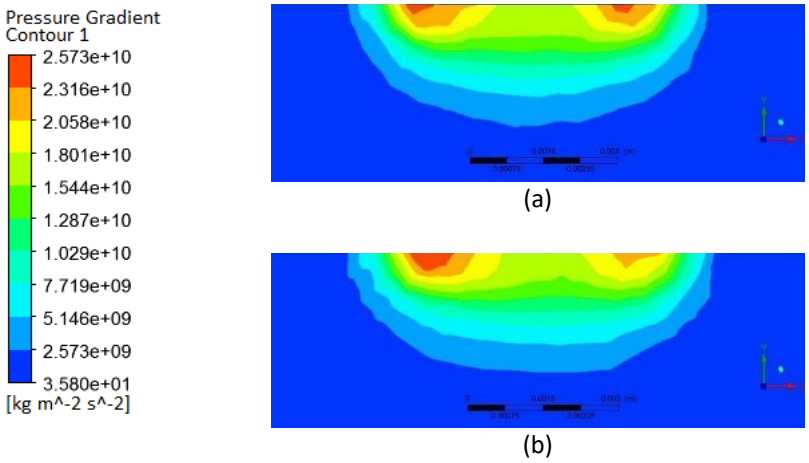

Fig. 15. Pressure gradient contour around leak region at 8 m/s (a) Leak 1 (b) Leak 2

Additionally, the turbulence kinetic energy (TKE) also changes owing to the turbulence effect in the leak region. The TKE contour at a fluid velocity of 8 m/s showed that the TKE around the leak region increased significantly. It rises from 3.595 x 10-4 J/kg to 1.106 x 104 J/kg, with the maximum occurring at the surface of the leak region and returning to the minimum when further away. The TKE can serve as an assisting parameter in leak detection systems to avoid false signal alarms. Figure 16 shows the TKE contour around the leak region at 8 m/s.

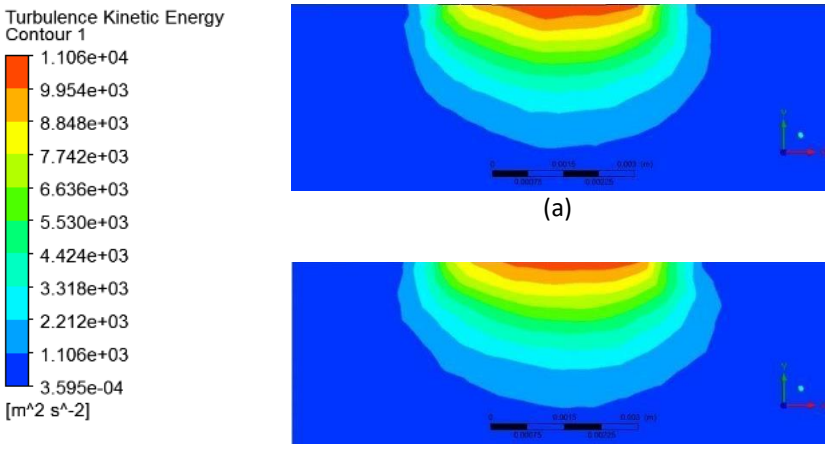

Fig. 16. Turbulence kinetic energy contour around leak region at 8m/s (a) Leak 1 (b) Leak 2

3.4.4 Flow behavior around the leaks at 9 m/s

First, the pressure distribution along the pipeline experienced disturbances at both Leaks 1 and 2, as shown in Figure 17. The distance between the two leaks is 2 meters. However, the pattern of pressure distribution is very similar for both leaks.

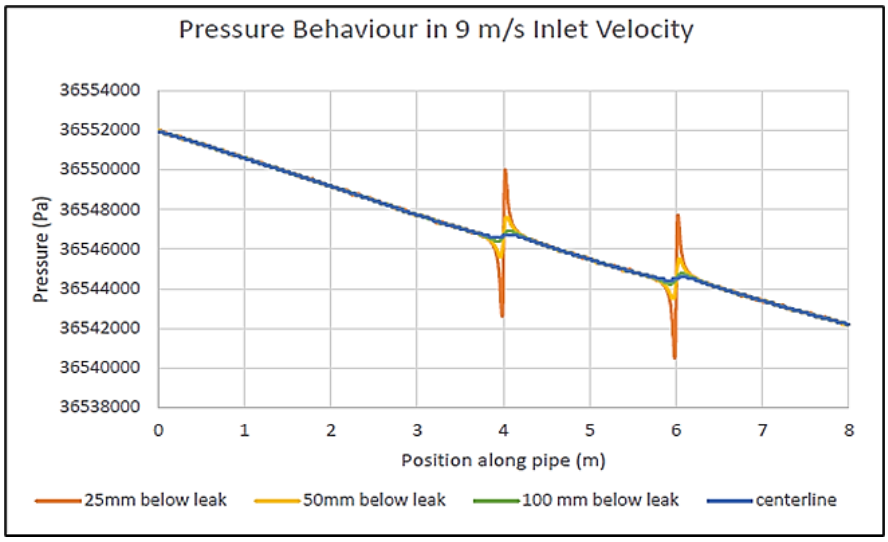

Fig. 17. Pressure distribution along pipeline for different positions at 9 m/s

From the graph above, the pressure behaviour 25 mm below the leak surface has the largest change in the pressure behaviour which gives the widest spike at both leaks. However, the pressure behaviour at the centre of the pipeline (161 mm) has the smallest spike which shows that there is a slight pressure change around the leaks. This shows that as the measurement moves away from the leak surface, the leakage signal becomes less noticeable.

From the pressure gradient contour above (Figure 18), there is a sudden change in the pressure around the leak region. The extreme change in the pressure gradient ranges from 4.147 X 10^{1} Pa/m to 2.571 X 10^{10} Pa/m at the entrance edge and exit edge of the leak, respectively. The pressure gradient can be used as data for the leak detection system to enhance the detection performance.

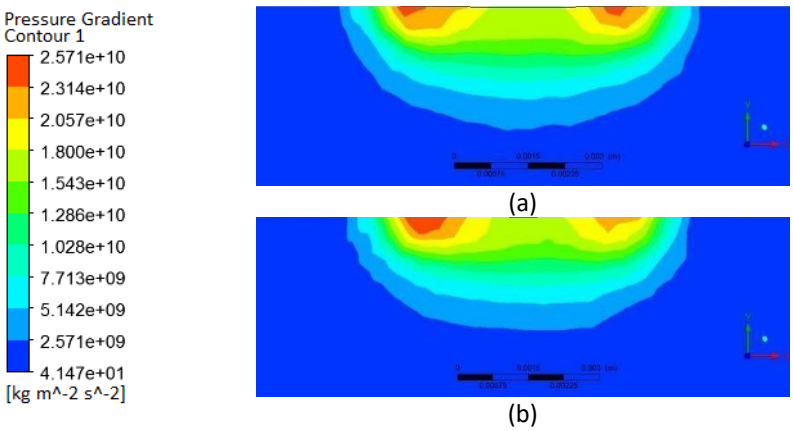

Fig. 18. Pressure gradient contour around leak region at 9 m/s (a) Leak 1 (b) Leak 2

In addition, the turbulence kinetic energy (TKE) of also experienced some changes owing to the turbulence effect in the leak region. The TKE contour at 9 m/s of fluid velocity shows that the TKE around the leak region increased significantly. It increased from 4.092 x 10-4 J/kg to 1.103 x 104 J/kg, with the maximum occurring at the surface of the leak region and back to the minimum when away from it. The TKE can be serve as an assisting parameter in the leak detection system to avoid false signal alarms. Figure 19 shows the TKE contour around the leak region at 9 m/s.

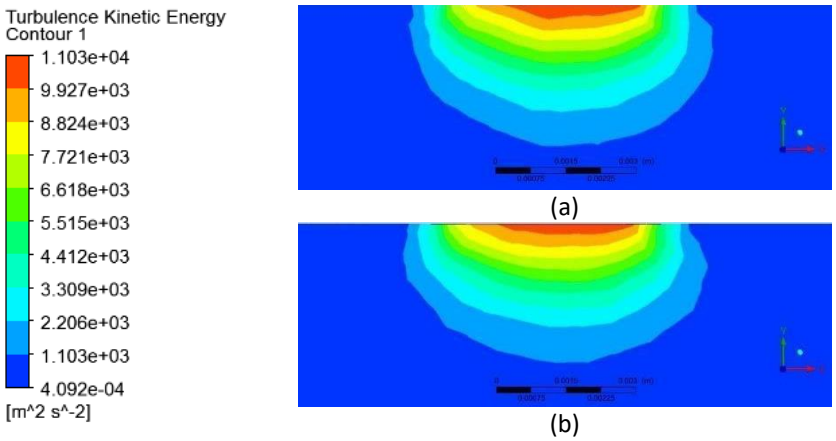

Fig. 19. Turbulence kinetic energy contour around leak region at 9 m/s (a) Leak 1 (b) Leak 2

3.5 Comparison of Pressure Behavior Between Different Distance Below the Leaks

Figures 20 to 23 show the relationship of the pressure behaviour around the leaks between different fluid velocities along the pipeline. A similar trend was observed in the pressure behaviour around the leaks for different fluid velocities. It is observed that the pressure distribution experienced a sudden drop and then increased to the maximum in the vicinity of the leak vigorously afterwards at both leaks 1 and 2. However, leak 2 at those four distances below the leakage shows a lower pressure compared to leak 1, because the velocity around leak 2 is higher than that around leak 1 according to Bernoulli's principle.

In addition, the fluctuation of pressure near the surface of the leakage (25 mm) is much more significant than the fluctuation of pressure at the centreline which is 161 mm from the surface of the leakages. Hence, this shows that as the measurement moves away from the leak surface, the leakage signal becomes less noticeable. This means that it is better to locate the detection sensor closer to the surface to identify the location of the leakage with better detectability.

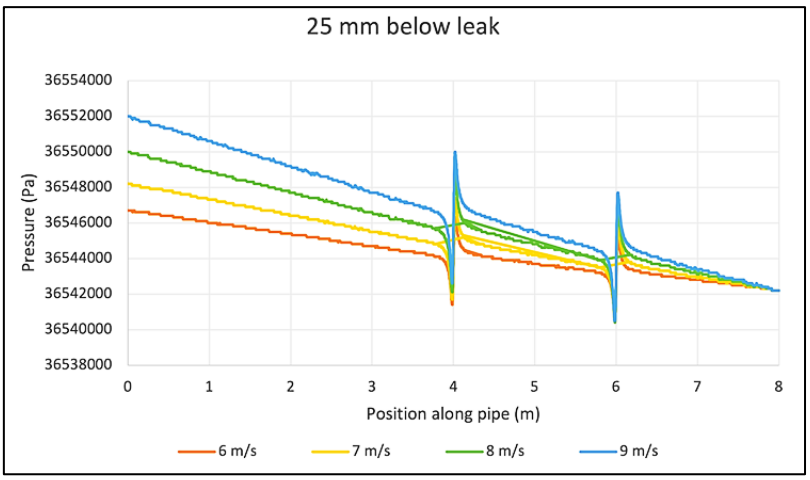

Fig. 20. Pressure behavior around the leaks between different fluid Velocity along the pipe at 25 mm below the leaks

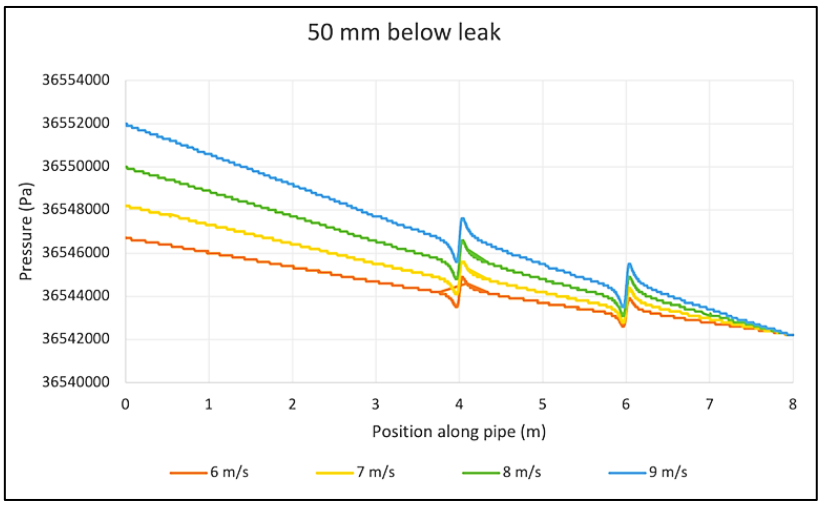

Fig. 21. Pressure behavior around the leaks between different fluid velocity along the pipe at 50 mm below the leaks

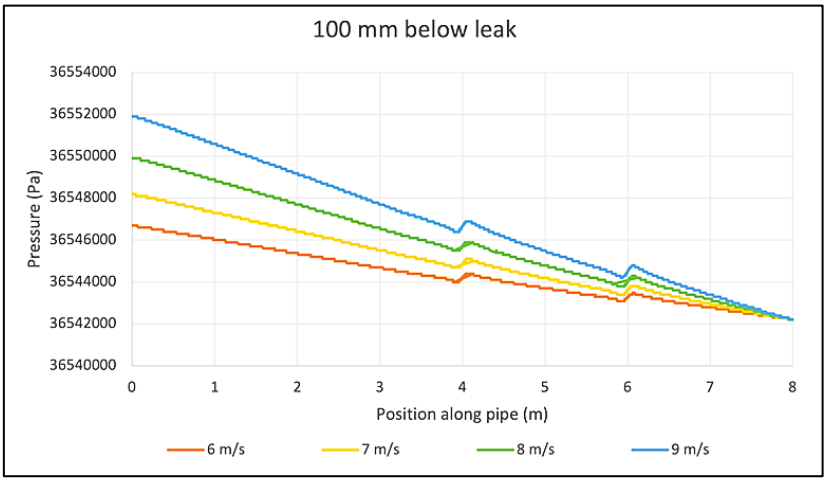

Fig. 22. Pressure behavior around the leaks between different fluid velocity along the pipe at 100 mm below the leaks

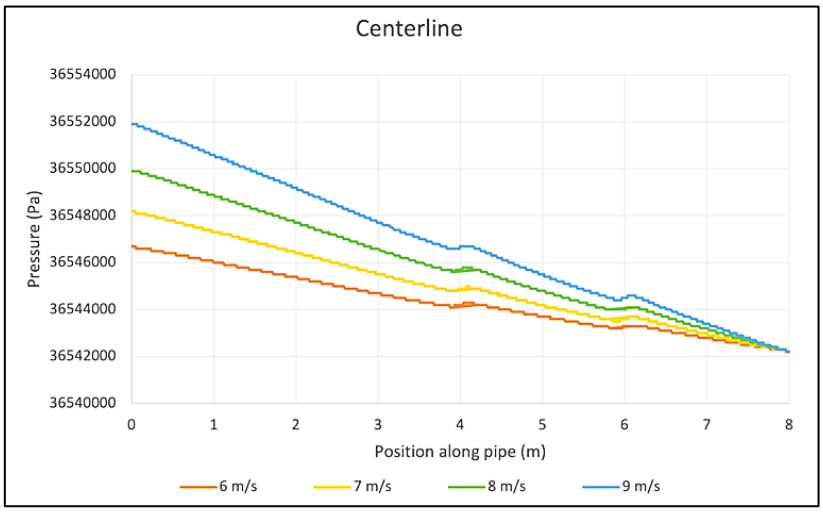

Fig. 23. Pressure behavior around the leaks between different fluid velocity along the pipe at centerline below the leaks

4. Conclusions

The objective of this study was to be successful. The effects of fluid velocity on the leak flow rate, pressure distribution, and turbulence kinetic energy around the leak regions were investigated. The study showed that as the fluid velocity increased, the leak flow rate of the pipeline also increased, and the leak at position 1 was consistently higher than that at position 2. Regarding the pressure behaviour around the leaks, a pattern of fluctuation occurs owing to turbulence in the leak regions at both leaks. However, the pressure fluctuation weakened as the measurement moved further from the leak point and closer to the pipe centreline. Hence, the second objective is successfully identified. A leak detection system should be installed near the surface of the pipeline, as this area exhibits the most significant changes in the pressure distribution when a leak occurs.

Acknowledgement

This research was supported by Universiti Tun Hussein Onn Malaysia (UTHM) through Tier 1 (vot Q449).

References

[1] Miranda, Stephany Medeiros, Carolina Andrade de Sousa, Ully Misse Moreno Benedito, and Oldrich Joel Romero. "Simulação numérica do transiente em dutos." Latin American Journal of Energy Research 3, no. 2 (2016): 21-29. https://doi.org/10.21712/lajer.2016.v3.n2.p21-29

[2] Kyriakides, Stelios, and Edmundo Corona. *Mechanics of Offshore Pipelines: Volume I: Buckling and collapse*. Gulf Professional Publishing, 2023.

[3] Reda, Ahmed, Ramy Magdy A. Mahmoud, Mohamed A. Shahin, Chiemela Victor Amaechi, and Ibrahim A. Sultan. "Roadmap for recommended guidelines of leak detection of subsea pipelines." *Journal of Marine Science and Engineering* 12, no. 4 (2024): 675. https://doi.org/10.3390/jmse12040675

[4] Wei, Ong Yong, and Siti Ujila Masuri. "Computational fluid dynamics analysis on single leak and double leaks subsea pipeline leakage." (2021).

[5] Munson, B.R., Young, D.F., Okiishi,T.H. and Huebsch, W.W., (2009). Fundamentals of Fluid Mechanics, 6th Edition, John Willey and Sons.

[6] Wang, Wenkang, Adrián Lozano-Durán, Rainer Helmig, and Xu Chu. "Spatial and spectral characteristics of information flux between turbulent boundary layers and porous media." *Journal of Fluid Mechanics* 949 (2022): A16. https://doi.org/10.1017/jfm.2022.770

[7] Šavli, Matic. "Turbulence kinetic energy–TKE." In *University of Ljubljana, Faculty of Mathematics and Physics, Department of Meteorology. Seminar: 4th Class. May*, vol. 27. 2012.

[8] Cassano, Katia, Alessio Pierro, Giovanna Froio, Raffaella Perini, Paolo Farinelli, Giuseppe De Marco, Cristina Amendola, and Alessio Caravella. "Modeling and simulation of multiphase high-pressure natural gas release from subsea pipelines due to possible breakage." In *Advances in Natural Gas: Formation, Processing, and Applications. Volume 6: Natural Gas Transportation and Storage*, pp. 333-359. Elsevier, (2024). https://doi.org/10.1016/B978-0-443-19225-8.00008-1

[9] Li, Xinhong, Yujiao Zhu, Jingwen Wang, Renren Zhang, and Guoming Chen. "Dispersion modeling of underwater oil released from buried subsea pipeline considering current and wave." *Ocean Engineering* 272 (2023): 113924. https://doi.org/10.1016/j.oceaneng.2023.113924

[10] Wang, Qiuyan, Yuling Lü, and Qigui Li. "A review on submarine oil and gas leakage in near field: Droplets and plume." *Environmental Science and Pollution Research* (2022): 1-14.

[11] Zhang, Yu, Shili Chen, Jian Li, and Shijiu Jin. "Leak detection monitoring system of long distance oil pipeline based on dynamic pressure transmitter." *Measurement* 49 (2014): 382-389. https://doi.org/10.1016/j.measurement.2013.12.009

[12] Agbakwuru, Jasper. "Oil/gas pipeline leak inspection and repair in underwater poor visibility conditions: challenges and perspectives." *Journal of Environmental Protection* 2012 (2012): 394-399 https://doi.org/10.4236/jep.2012.35049

[13] Sandberg, Chet, Jim Holmes, Ken McCoy, and Heinrich Koppitsch. "The application of a continuous leak detection system to pipelines and associated equipment." *IEEE Transactions on Industry Applications* 25, no. 5 (1989): 906-909. https://doi.org/10.1109/28.41257

[14] Adegboye, Mutiu Adesina, Wai-Keung Fung, and Aditya Karnik. "Recent advances in pipeline monitoring and oil leakage detection technologies: principles and approaches." *Sensors* 19, no. 11 (2019): 2548. https://doi.org/10.3390/s19112548

[15] Cham, Alhagie, and Meraj Mustafa. "Boundary layer formations over a stretchable heated cylinder in a viscoelastic fluid with partial slip and viscous dissipation effects." *Numerical Heat Transfer, Part A: Applications* 85, no. 11 (2024): 1767-1779. https://doi.org/10.1080/10407782.2023.2210259

[16] Razvarz, Sina, Raheleh Jafari, and Alexander Gegov. "Flow modelling and control in pipeline systems." *Stud. Syst. Decis. Control* 321 (2021): 25-57. https://doi.org/10.1007/978-3-030-59246-2_2

[17] Sekhavati, Javad, Seyed Hassan Hashemabadi, and Masoud Soroush. "Computational methods for pipeline leakage detection and localization: A review and comparative study." *Journal of Loss Prevention in the Process Industries* 77 (2022): 104771. https://doi.org/10.1016/j.jlp.2022.104771

[18] Jujuly, Muhammad, Premkumar Thodi, Aziz Rahman, and Faisal Khan. "Computational fluid dynamics modeling of subsea pipeline leaks in arctic conditions." In *OTC Arctic Technology Conference*, pp. OTC-27417. OTC, 2016. https://doi.org/10.4043/27417-MS

[19] Harolanuar, Muhammad Nur Hanafi, Nurul Fitriah Nasir, Hanis Zakaria, and Ishkrizat Taib. "Analysis of fluid flow on the n95 facepiece filtration layers." *Journal of Advanced Research in Fluid Mechanics and Thermal Sciences* 100, no. 1 (2022): 172-180. https://doi.org/10.37934/arfmts.100.1.172180

[20] Taib, Ishkrizat. "Analysis of electromagnetic waves differences in hyperthermia." *Journal of Industry, Engineering and Innovation* 5, no. 1 (2023): 5-10.